Zuse Institute Berlin

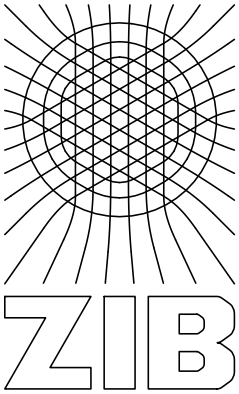

Takustr. 7
14195 Berlin
Germany

RALF LENZ AND ROBERT SCHWARZ

Optimal Looping of Pipelines in Gas Networks

ZIB Report 16-67 (December 2016)

Zuse Institute Berlin
Takustr. 7
14195 Berlin
Germany

Telephone: +49 30-84185-0
Telefax: +49 30-84185-125

E-mail: bibliothek@zib.de
URL: http://www.zib.de

ZIB-Report (Print) ISSN 1438-0064
ZIB-Report (Internet) ISSN 2192-7782

Optimal Looping of Pipelines in Gas Networks

Ralf Lenz and Robert Schwarz

{lenz, schwarz}@zib.de

December 22, 2016

Abstract

In this paper, we compare several approaches for the problem of gas network expansions using loops, that is, to build new pipelines in parallel to existing ones. We present different model formulations for the problem of continuous loop expansions as well as discrete loop expansions. We then analyze problem properties, such as the structure and convexity of the underlying feasible regions. The paper concludes with a computational study comparing the continuous and the discrete formulations.

1. Introduction

Gas transmission operators own and operate the pipeline network infrastructure. They are faced with both increasing demand and the need to handle more diverse transport situations. In order to keep up, they need to expand their network's capacity. This is known as Expansion Planning and can be modeled as a nonconvex Mixed-Integer Nonlinear Program (MINLP), where discrete decisions correspond to the operation of active network elements and nonlinear constraints are needed to model the flow-pressure relationship in pipes. Building new pipes in parallel to existing ones, also called looping, is a popular method to increase throughput in practice.

It is still an open research topic to choose the right expansion candidates, since a single method like looping provides no guarantee for feasibility. Fügenschuh and Humpola present a bottleneck analysis in [HF15] that helps to find out whether an infeasible flow situation can be resolved with loop expansions. For an literature overview about different expansion planning approaches, we refer the reader to [RMBS15], [BBB$^+$15] or [BNV12].

In section 2, we present formulations for two different kind of loop expansion problems. At first we formalize the problem of dealing with continuous loop lengths, called

split-pipe problem in the literature, as well as the appropriate choice of loop diameters out of a discrete set. Since it is possible to determine the best looping diameters a priori, we can efficiently reduce the problem size of the resulting MINLP. We also present the problem of discrete loop expansions, that is to decide whether a pipe is looped over its full length or not all.

In section 3, we compare the feasible regions of the split-pipe and discrete approach. In section 4, we highlight problem properties, such as the nonconvexity of the split-pipe and discrete formulation and give an example that the Braess' paradox is also valid in the context of loop expansions. We conclude with a computational study comparing the split-pipe and discrete formulations.

2. Modeling Gas Network Loop Expansions

A gas network is represented by a directed graph $\mathcal{G} = (\mathcal{V}, \mathcal{A})$, where the set of nodes $\mathcal{V}$ consists of sources, sinks and intermediate nodes and the arc set $\mathcal{A}$ comprises pipes, compressor stations, valves, control valves and resistors. In this paper, we only consider passive gas networks, that is, all arcs are pipe segments. A nomination is given by $b \in \mathbb{R}^{|\mathcal{V}|}$, where $b_v > 0, b_v < 0$ denotes injection into and withdrawal from the network at node $v \in \mathcal{V}$, otherwise $b_v = 0$. Since we work with stationary gas flow models, the nominations are balanced and we have $\sum_{v\in\mathcal{V}} b_v = 0$. Flow mass balance is required at every node:

$$\sum_{a\in\delta^+(v)} x_a - \sum_{a\in\delta^-(v)} x_a = b_v, \quad \forall v \in \mathcal{V}.$$

The physical state of the network is described by bounded pressure variables $p_v \in [\underline{p}_v, \overline{p}_v] \,\forall\, v \in V$ and flow variables $x_a \in [\underline{x}_a, \overline{x}_a] \,\forall\, a \in A$.

The transported amount of gas leads to a pressure loss in each arc $a \in \mathcal{A}$ along the flow direction and is represented by the Weymouth equation:

$$p_v^2 - p_w^2 = \frac{L_a K_a}{D_a^5} x_a |x_a| \qquad \forall a = (v, w) \in \mathcal{A}, \text{ with} \tag{1}$$

D_a	diameter of pipe a
L_a	length of pipe a
K_a	physical constant of pipe a.

For more details about different approaches of modeling and solving gas network nominations, we refer the reader to chapter 6 - 9 in [KHPSe15] and for the approximation of the underlying gas physics in pipes by the Weymouth equation to [Wey12]. We assume here that all pipes are located on a flat surface with zero slope, that is, there is no influence of gravity on the pressure drop. Since the pressure variables only appear in the quadratic form of (1), we subsequently replace them by $\pi = p^2$, with bounds $\pi \in [\underline{p}^2, \bar{p}^2]$.

This model forms the base for the following approaches of modeling loop expansions.

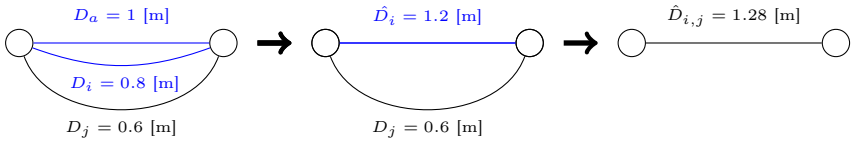

Figure 1: Example for the calculation of an equivalent diameter, where $\hat{D}_i = eq(D_a, D_i)$ and $\hat{D}_{i,j} = eq(\hat{D}_i, D_j)$.

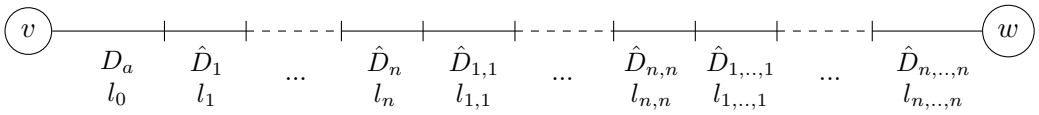

Figure 2: Possible diameter allocation of a looped pipe.

2.1. Split Pipe Loop Expansions

We are given a finite set $\mathcal{D} = \{D_1, \ldots, D_n\}$ containing the diameter candidates for the loops of a pipe. The diameters $\mathcal{D}$ are associated with costs, see figure 3. We allow a single pipe to be looped up to r times with any possible combination of diameters of $\mathcal{D}$. We do this by calculating the equivalent diameters $\hat{D}$ of the original diameter D_a and $D_i, i \in \{1, ..., n\}$ in the following:

$$\hat{D}_i := eq(D_a, D_i) = \left(D_a^{5/2} + D_i^{5/2}\right)^{2/5} \qquad \forall i \in \{1, ..., n\}$$
$$\hat{D}_{i_1,...,i_r} := eq(\hat{D}_{i_1,...,i_{r-1}}, D_{i_r}) \qquad \forall i_1, \ldots, i_r \in \{1, ..., n\}.$$

Note that a derivation of the formula is given in the appendix A and B. An example for the calculation of an equivalent diameter for an original pipe with two loops is provided for normalized pipe length in figure 1. Since the equivalent diameter is commutative, it follows that $\hat{D}_{i,j} = \hat{D}_{j,i}$.

Each equivalent diameter $\hat{D}$ has a corresponding continuous variable $l \in [0, 1]$ that represents its partial loop length, that is, the relative length of the pipe segment using this diameter. Figure 2 illustrates that a pipe can basically be looped with all possible combinations of equivalent diameters. Thus, this model can be viewed as a relaxation to approaches where a single diameter is chosen to be looped over the full pipe length, as done in [Hum14].

We then apply a model reduction following [FD87]. We restrict the number of equivalent diameters to a small set, while being able to represent the capacity of the neglected ones. To this end, we consider the cost factor C over a power function of the equivalent diameters, shown in Figure 4. This function of the diameter corresponds to the impact that the diameter has on the pressure loss in equation (1).

Subsequently we calculate the lower part of the convex hull of these values, see the red line segments in Figure 4. Optimal loop diameters then correspond to extreme points of this lower part of the convex hull. For a proof, we refer to [FD87]. Hence, we eliminate all equivalent diameters that are not extreme points. In the following

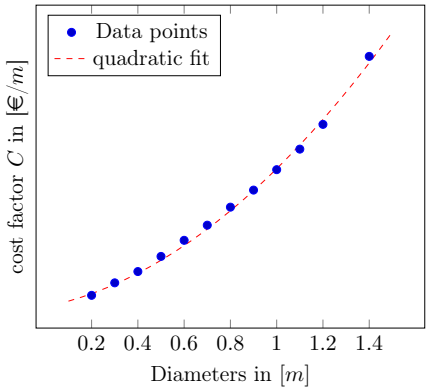

Figure 3: Diameter candidates.

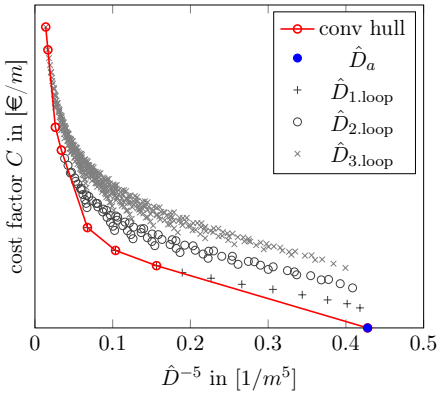

Figure 4: "Lower part" of the convex hull.

we denote the set of equivalent diameters of a pipe a that corresponds to the extreme points of the "lower part" of the convex hull in descending order $\{\hat{D}_{a,0}, ..., \hat{D}_{a,k_a}\}$ with length variables $l_{a,0}, ..., l_{a,k_a}$. Here, $\hat{D}_{a,0}$ typically corresponds to the (unlooped) diameter D_a of the existing pipe. A tuple $(\hat{D}_{a,i}, l_{a,i})$ indicates the proportion of how much the "associated factor" $(L_a K_a / \hat{D}_{a,i}^5) l_{a,i}$ contributes to the overall pressure loss of the pipe, see equation (2b). Since the cost factor C is a strictly convex function over the extreme points, optimal solutions have the property that pipes are looped by at most two different and adjacent diameters. That is, the $l_{a,i}$ variables implicitly form a special ordered set of type 2.

Our approach is similar to that of [ZZ96] for the optimal pipe dimensioning problem, where they also use continuous variables to represent the relative length of segments using different diameters. The difference is that we extend it by accounting for the impact of equivalent diameters that represent multiple loops of diameters out of the candidate set.

With these insights we build the following formulation. The objective function is to minimize the costs of the built loops (2a). Modeling loops is integrated in the nonconvex and nonlinear equation (2b). The segments must cover the complete pipe length by (2c).

$$\underset{l,x,\pi}{\text{minimize}} \quad \sum_{a \in \mathbb{A}} \left(L_a \sum_{i=0}^{k_a} l_{a,i} C(\hat{D}_{a,i}) \right) \tag{2a}$$

$$\text{subject to} \quad \pi_v - \pi_w = L_a K_a \left(\sum_{i=0}^{k_a} \frac{l_{a,i}}{\hat{D}_{a,i}^5} \right) x_a |x_a| \qquad \forall\, a = (v,w) \in A \tag{2b}$$

$$\sum_{i=0}^{k_a} l_{a,i} = 1 \qquad \forall\, a \in A \tag{2c}$$

$$\sum_{a \in \delta^+(v)} x_a - \sum_{a \in \delta^-(v)} x_a = b_v \qquad \forall\, v \in V \tag{2d}$$

$$\underline{\pi}_v \leq \pi_v \leq \overline{\pi}_v \qquad \forall\, v \in V \tag{2e}$$

$$\underline{x}_a \leq x_a \leq \overline{x}_a \qquad \forall\, a \in A \qquad (2f)$$
$$l_{a,i} \in [0,1] \qquad \forall\, a \in A\, \forall i \in [k_a] \qquad (2g)$$

with

$\hat{D}_{a,0}, ..., \hat{D}_{a,k_a}$	equivalent diameters of pipe a
	= extreme points of the "lower part" of the convex hull
$l_{a,i}$	relative length of pipe segment with $\hat{D}_{a,i} \in \{\hat{D}_{a,0}, ..., \hat{D}_{a,k_a}\}$

2.1.1. Alternative Formulation for Split Pipe Loop Expansions

In the previous section, we modeled the "lower part" of the convex hull (see figure 4) using length variables l_i. Here, we present an alternative approach to formulate the split-pipe model by imposing this "lower part" of the convex hull with linear constraints. For that purpose, we introduce a variable $c_{a,i}$ that represents the costs of pipe a with equivalent diameter $\hat{D}_{a,i}$ and add linear constraints (3b) for all adjacent pairs of extreme points that span the "lower part" of the convex hull, see figure 5b. These cuts can be added globally or on the fly when ever an LP solution violates these cuts.

$$\begin{aligned}
\underset{y,c,x,\pi}{\text{minimize}} \quad & \sum_{a \in \mathbb{A}} c_a \\
\text{subject to} \quad & \pi_v - \pi_w = L_a K_a y_a\, x_a |x_a| && \forall\, a = (v,w) \in A && (3a)\\
& \sum_{a \in \delta^+(v)} x_a - \sum_{a \in \delta^-(v)} x_a = b_v && \forall\, v \in V \\
& c_a \geq s_{a,i} y_{a,i} + t_i && \forall a \in A\, \forall i \in [k_a - 1] && (3b)\\
& \underline{\pi}_v \leq \pi_v \leq \overline{\pi}_v && \forall\, v \in V \\
& \underline{x}_a \leq x_a \leq \overline{x}_a && \forall\, a \in A \\
& \underline{y}_a \leq y_a \leq \overline{y}_a && \forall\, a \in A
\end{aligned}$$

where (3b) is explicitly given by

$$\begin{aligned}
s_{a,i} &:= \frac{c_i - c_{i+1}}{(\hat{D}_{a,i}^{-5} - \hat{D}_{a,i+1}^{-5})} \\
t_{a,i} &:= -s_{a,i} \hat{D}_{a,i+1}^{-5} + c_{i+1},
\end{aligned}$$

and $\underline{y}_a := \hat{D}_{a,k_a}^{-5}$, $\overline{y}_a := \hat{D}_{a,0}^{-5}$. Note that $(\hat{D}_{a,i}^{-5}, c_{a,i})$ correspond to the extreme points of the "lower part" of the convex hull, as shown in figures 5a and 5b.

Both formulations 2.1 and 2.1.1 are equivalent in that they yield the same optimal solutions. The only difference is in the constraints (2b), (2c) and respectively (3b). In principle, the feasible region of these constraints is depicted in the gray shaded area of figures 5a and 5b. But since the objective is to minimize the costs, the solution is forced to be on the "lower part" of the convex hull for the l_i variables in formulation 2.1 as well as for the y variables in formulation 2.1.1.

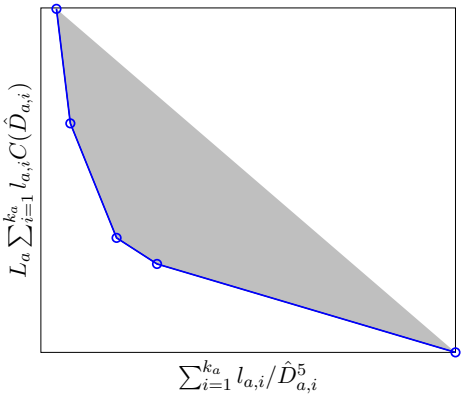

(a) Feasible region of $l_{a,i}$-variables in formulation (2).

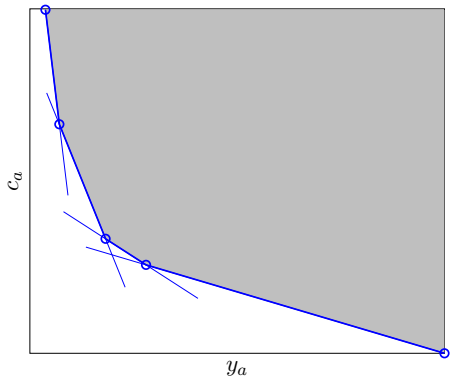

(b) Feasible region of y_a-variables in formulation (3).

Figure 5: Feasible regions.

2.2. Discrete Loop Expansions

Most approaches in the literature rely on the usage of binary variables to indicate if a pipe is looped over the full pipe length with a certain diameter or not looped at all. Such a discrete approach can be applied to the case of several loops for an existing arc, as done in [Hum14]. Humpola defines an extended arc set $\mathcal{A}_X \subset \mathcal{A} \times \mathbb{N}_{\geq 0}$ and allows a pipe to be looped up to n times with the original diameter. To this end, binary variables are introduced for each arc $(a, i) \in \mathcal{A}_X$ to model the decision that arc (a, i) is used, which means that arc a is looped i times with its original diameter.

For comparison purposes between a split-pipe and discrete formulation of loop expansions, we modify the formulation of [Hum14] by allowing a pipe to be fully looped up to r times with any diameter combination out of the candidate set $\mathcal{D} = \{D_1, \ldots, D_n\}$. As described in section 2.1, we compute the same extreme points that correspond to the "lower part" of the convex hull in descending order $\{\hat{D}_{a,0}, ..., \hat{D}_{a,k_a}\}$. Due to equation (4e), exactly one binary variable $z_{a,i}$ is selected that chooses one difference of squared pressure variable $\Delta_{a,i}$ in the big M-formulation (4d) to be non-zero and hence selects the corresponding equivalent diameter in equation (4b).

$$\underset{z,x,\Delta,\pi}{\text{minimize}} \quad \sum_{a \in \mathbb{A}} L_a \sum_{i=0}^{k_a} C(\hat{D}_{a,i}) z_{a,i} \tag{4a}$$

$$\text{subject to} \quad x_a |x_a| - \sum_{i=0}^{k_a} \frac{\hat{D}_{a,i}^5}{L_a K_a} \Delta_{a,i} = 0 \qquad \forall\, a \in A, \tag{4b}$$

$$\sum_{i=0}^{k_a} \Delta_{a,i} - (\pi_v - \pi_w) = 0 \qquad \forall\, a = (v, w) \in A, \tag{4c}$$

$$-M\, z_{a,i} \leq \Delta_{a,i} \leq M\, z_{a,i} \qquad \forall a \in A\ \forall i \in [k_a], \tag{4d}$$

$$\sum_{i=0}^{k_a} z_{a,i} = 1 \qquad \forall\, a \in A, \tag{4e}$$

$$\sum_{a\in\delta^+(v)} x_a - \sum_{a\in\delta^-(v)} x_a = b_v \qquad \forall\, v \in V, \tag{4f}$$

$$\underline{\pi}_v \le \pi_v \le \overline{\pi}_v \qquad \forall\, v \in V, \tag{4g}$$

$$\underline{x}_a \le x_a \le \overline{x}_a \qquad \forall\, a \in A, \tag{4h}$$

$$z_{a,i} \in \{0,1\} \qquad \forall a \in A\ \forall i \in [k_a]. \tag{4i}$$

with

$\hat{D}_{a,0}, ..., \hat{D}_{a,k_a}$	equivalent diameters of pipe a
	= extreme points of the "lower part" of the convex hull
$z_{a,i}$	decision to build pipe a with equivalent diameter $\hat{D}_{a,i}$
$\Delta_{a,i}$	squared pressure loss of pipe a with equivalent diameter $\hat{D}_{a,i}$

3. Comparison of the Feasible Regions

In the following, we denote the feasible region of the split-pipe or discrete model and their relaxations or modifications, as:

- X_{sp} - feasible region of the split-pipe model (2)
- $X_{sp,bin}$ - feasible region of the integral split-pipe model, i.e. setting all variables $l_{a,i}$ to be binary in model (2)
- X_{disc} - feasible region of the discrete model (4)
- $X_{disc,rel}$ - feasible region of the continuous relaxation of model (4)

In this section, we show the three relations highlighted in figure 6. The other relations $X_{sp,bin} \subseteq X_{sp}$ and $X_{disc} \subseteq X_{disc,rel}$ are evident, since they are the canonical continuous relaxations of the integral variables.

Since the different model formulations do not share the same variables, the set inclusion does not hold literally. Instead, we understand inclusion to mean that a suitable mapping of feasible points exists.

Proposition 1. *The continuous relaxation of the discrete model* (4) *is weaker than the split-pipe model* (2)*, i.e.* $X_{sp} \subseteq X_{disc,rel}$.

Proof. Given a solution of model (2), i.e. a solution vector $\left(\tilde{x}_a, \tilde{\pi}_v, \tilde{l}_{a,i}\right)_{a\in A, v\in V, i\in[k_a]} \in X_{sp}$. We show, that it can be transformed to a point in $X_{disc,rel}$. To this end, we set for all pipes $a \in A$: $x_a := \tilde{x}_a$, $\pi_v := \tilde{\pi}_v$ and $z_{a,i} := \tilde{l}_{a,i}\, \forall i \in [k_a]$. With this assumption, equations (4e), (4f) hold as well as the variable bounds (4g)-(4h). Define

$$\Delta_{a,i} := z_{a,i} x_a |x_a| \frac{L_a K_a}{\hat{D}_{a,i}^5} \qquad \forall a \in A\ \forall i \in [k_a] \tag{5}$$

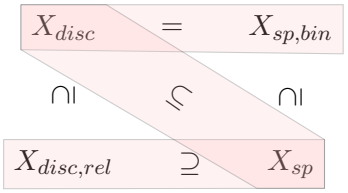

Figure 6: Relation of feasible regions.

$$\Rightarrow \sum_{i=0}^{k_a} \Delta_{a,i} \overset{(5)}{=} x_a|x_a| \sum_{i=0}^{k_a} z_{a,i} \frac{L_a K_a}{\hat{D}_{a,i}^5} \overset{(2b)}{=} \pi_v - \pi_w \qquad \forall a \in A, \tag{6}$$

and thus the pressure loss constraint (4c) is satisfied. Setting $M \geq x_a|x_a|L_aK_a/\hat{D}_{a,0}^5$, then the big M-formulation (4d) holds by construction. Equation (4b) also holds, since

$$\begin{aligned}
&\overset{(5)}{\Rightarrow} z_{a,i} x_a|x_a| = \frac{\hat{D}_{a,i}^5}{L_a K_a} \Delta_{a,i} && \forall a \in A\, \forall i \in [k_a], \\
&\Rightarrow \sum_{i=0}^{k_a} z_{a,i} x_a|x_a| = \sum_{i=0}^{k_a} \frac{\hat{D}_{a,i}^5}{L_a K_a} \Delta_{a,i} && \forall a \in A, \\
&\overset{(4e)}{\Rightarrow} x_a|x_a| = \sum_{i=0}^{k_a} \frac{\hat{D}_{a,i}^5}{L_a K_a} \Delta_{a,i} && \forall a \in A.
\end{aligned}$$

□

Note that the reverse is not true, i.e. $X_{disc,rel} \not\subseteq X_{sp}$. Instead of providing a counterexample, we refer to the computational experiments shown in table 5 of the appendix. The results illustrate that the optimal objective value is better for the continuous relaxation of the discrete model than for the split-pipe model.

But formulations (2) and (4) are equivalent when restricting the continuous length variables in (2) to be binary, as described in proposition 2.

Proposition 2. *Restricting the continuous variables to be binary $l_{a,i} \in \{0,1\}$ for all $a \in A$ and for all $i \in [k_a]$ in the split-pipe model* (2)*, results in a feasible region that equals the one of the discrete model* (4)*, that is, $X_{sp,bin} = X_{disc}$.*

Proof. "$X_{sp,bin} \subseteq X_{disc}$":
Let $\left(\tilde{x}_a, \tilde{\pi}_v, \tilde{l}_{a,i}\right)_{a\in A, v\in V, i\in[k_a]} \in X_{sp}$ be a solution of formulation (2), that also fulfills $\tilde{l}_{a,i} \in \{0,1\}$. Again, we set for all pipes $a \in A$ and $\forall i \in [k_a]$: $x_a := \tilde{x}_a$, $\pi_v := \tilde{\pi}_v$ and $z_{a,i} := \tilde{l}_{a,i}$. Then equations (4f)-(4h) follow right away and equation (4e) holds because of equation (2c). For pipe a let $\breve{i}_a \in [k_a]$ be such that $\tilde{l}_{a,\breve{i}_a} = 1$. We define

$$\Delta_{a,i} := \begin{cases} 0 & \forall i \in [k_a] \setminus \breve{i}_a \\ \frac{L_a K_a}{\hat{D}_{a,i}^5} x_a|x_a| & i = \breve{i}_a. \end{cases} \tag{7}$$

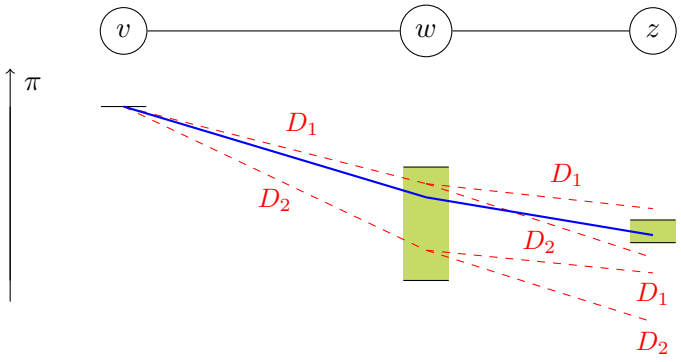

Figure 7: Example of a graph with given pressure bounds, where the split-pipe model has a solution (blue) and the discrete model is infeasible (red dashed lines).

Then equation (4b) follows by construction, equation (4c) equals equation (2b) and equation (4d) holds by setting $M \geq \Delta_{a,\check{i}_a}$.

"$X_{disc} \subseteq X_{sp,bin}$":

Let $(x_a, \pi_v, z_{a,i}, \Delta_{a,i})_{a \in A, v \in V, i \in [k_a]} \in X_{disc}$ be a solution of model (4). We set for all pipes $a \in A$ and $\forall i \in [k_a] : \tilde{x}_a := x_a$, $\tilde{\pi}_v := \pi_v$ and $\tilde{l}_{a,i} := z_{a,i}$. Then equation (2c) holds because of (4e) and equation (2b) follows from equations (4b) - (4d). □

Proposition 3. *The split-pipe model* (2) *is a relaxation of the discrete model* (4)*, i.e.* $X_{disc} \subseteq X_{sp}$.

Proof. It follows directly from proposition 2, since $X_{disc} = X_{sp,bin}$ and $X_{sp,bin} \subseteq X_{sp}$. □

4. Problem Properties

4.1. Feasibility of Models

It is an interesting theoretical question, whether there are instances that are only feasible for the split-pipe model but infeasible for the discrete model. The following simple example provides such a situation, which is induced by different pressure bounds at the nodes.

Example Figure 7 shows a graph with three nodes v, w, z and two arcs $(vw), (wz)$. The squared pressure variable at node v is fixed to its upper bound and the squared pressure intervals of nodes w and z are highlighted in green. Assume a certain demand situation to be given. Both pipes can be laid out with one of the two diameter candidates D_1 or D_2. While any diameter combination for the two pipes in the discrete case cannot meet the squared pressure range at node z, the split-pipe model does so by an appropriate convex combination of the diameters for both pipes.

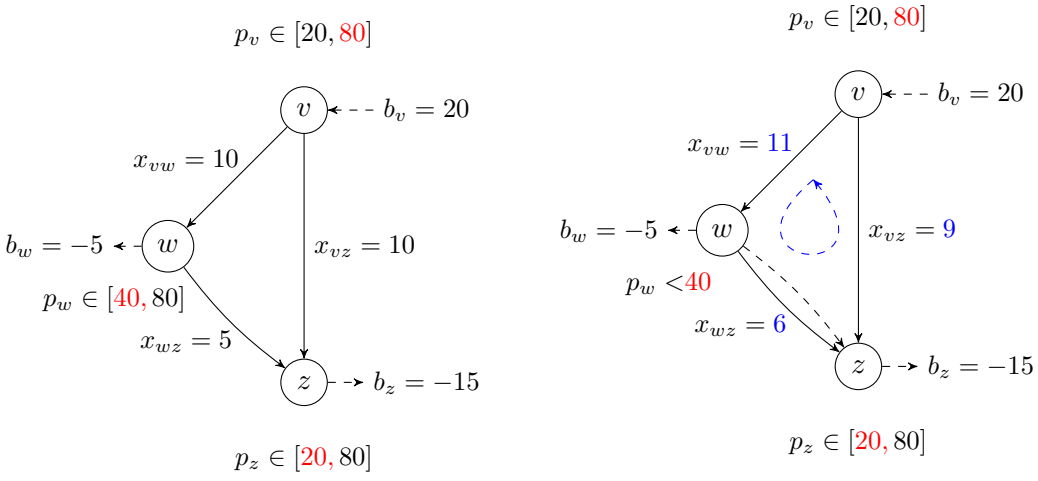

(a) Feasible network state, where the pressures of all nodes are at the bounds (red values).

(b) Looping pipe wz (black dashed line) turns the network state infeasible. More gas flows now in the direction of the blue dashed line.

Figure 8: Braess phenomenon in the context of looping gas networks.

4.2. Braess' Paradox

In the context of road networks, Braess discovered that potential improvements of traffic flows, e.g., opening new streets, could lead to a deterioration of the travel time[Bra68]. This effect is called Braess' paradox. It is a counterexample to the monotonicity assumption that more network capacity leads to more throughput. This paradox is also known in gas network expansion planning, e.g. as "more pipeline - less throughput phenomenon", when adding a new element to the gas network might lead to infeasibility, see [Sza12]. Here we provide an example that this phenomenon also may occur in the context of looping, see figure 8. A feasible network flow situation turns infeasible just by doubling pipe wz. This is because the pressure variables of the nodes are already at the bounds (fig. 8a). Adding the loop now changes the flow situation in the sense that more gas flows along the looped pipe wz and therewith through pipe vw, yielding a violation of the lower pressure bound at node w (fig. 8b). Note that this example requires non-uniform pressure bounds on the nodes.

4.3. Convexity Analysis

In [HF15], Humpola et al. proved convexity of the feasible region with respect to flow and node potential variables (x, π) of the so-called domain relaxation problem for passive networks as described in section 2. The proof relies on the fact that the flow distribution is uniquely defined and the projection on the π-variables is unique up to a constant shift within an interval, which was shown by [Mau77].

The interesting fact is that even though the problem comprises nonlinear nonconvex constraints, such as equation (1), its feasible region is convex. But this property does not

hold for the feasible regions of both split-pipe and discrete expansion planning problem. Both problems have a nonconvex feasible region. While it is obvious for the discrete problem due to its discrete nature of the binary variables, we provide an example that shows the nonconvexity of the feasible region of the split-pipe problem.

Counterexample Consider a network of two pipes, as shown in figure 14 and the corresponding model. Given a demand situation $b_t = 121$ and $b_h = -121$, the physical properties of the pipes are such that $y_1 = 1$ and $y_2 = 0.01$ and the bounds of the squared pressure variables are: $\pi_t^2 - \pi_h^2 \in [10, 140]$. For a given flow situation in parallel pipes, the flow distribution among the parallel pipes is unique and described by equation (11) in appendix A. Hence, we get a feasible pressure loss $\pi_t^2 - \pi_h^2 = 121$ with $x_1 = 11$ and $x_2 = 110$. Projecting the solution onto the (y_1, y_2)-space, we have two feasible solutions: $y = (0.01, 1)$ and $\tilde{y} = (1, 0.01)$, by symmetry. But a convex combination of y and $\tilde{y}$, such as $0.5(y + \tilde{y}) = (0.505, 0.505)$ is infeasible, since equation (11) yields $x_1 = 60.5$ and $\pi_t^2 - \pi_h^2 = y_1 x_1^2 = 0.505 \cdot 60.5^2 > 140$.

5. Computational Study

In this section, we computationally compare the discrete expansion problem with the split-pipe expansion problem. We conduct two experiments: At first, we compare the continuous relaxation of the discrete model 2.2 with the split-pipe model 2.1. The latter one can also be seen as a relaxation of the discrete model. For a fair comparison, we examine how close the dual bound in the root node of both relaxations comes to the optimal value of the discrete model.

Secondly, we compare the discrete problem with the split-pipe problem in the tree search, considering a time-limit of five hours per instance. Especially for practical purposes it is an important question, whether cost savings of the split-pipe loop expansions are significant compared to the approach of discrete loop expansions.

We implemented these models in ZIMPL [Koc04] using SCIP as MINLP solver ([Ach09] and [Vig12]).

5.1. Implementation Details

A drawback of the split-pipe formulations (2) and (3) is, that a further quadratic constraint has to be introduced for each pipe: $\pi_v - \pi_w = y_a z_a$, since SCIP cannot take advantage of the structure of constraint type (2b) or (3a). On the other hand, this additional nonlinearity does not depend on the number of extreme points, since it is independent of the number k_a in formulation (2) or rather independent of the number of linear constraints in formulation (3). Subsequently, we illustrate how SCIP handles

equation (2b). It is split into constraints of types abspower, quadratic and linear:

$$\pi_v - \pi_w = \underbrace{\underbrace{L_a C \left(\sum_{i=0}^{k_a} \frac{l_{a,i}}{\hat{D}_{a,i}^5} \right)}_{=y_a \text{ linear}} \underbrace{x_a |x_a|}_{=z_a \text{ abspower}}}_{y_a \cdot z_a \text{ quadratic}}.$$

The advantage of the discrete model (4) is that these additional quadratic constraints are avoided. This is due to the fact, that the model formulation allows to account for the impact of the equivalent diameters on the side of the difference of squared pressure variables, see equation (4b). However an obvious drawback of model (4) is the existence of binary variables. In the following computational experiments, we use formulation (2) as representation of the split-pipe model.

5.2. Experimental Setup

Test set We randomly generated 52 instances based on the Belgium gas network, where the network data is publicly available at [DWS00] or [Lib]. We slightly modified this network, exactly as done in [HFK16], by substituting all active elements for pipes. Additionally we added several new pipelines to the network to create more cycles, which increase the network complexity. The demand vectors are randomly generated, such that the same nodes are always sources, sinks or innodes, in accordance with [Lib].

Hardware and Software The experiments are conducted on a cluster of 64bit Intel Xeon E5-2680 CPUs at 2.7GHz with 20MB cache and 64GB main memory. In order to safeguard against a potential mutual slowdown of parallel processes, we ran only one job per node at a time. We used SCIP version 3.2.1 with CPLEX 12.6 as LP solver and Ipopt 3.12.6 as NLP solver.

5.3. Root Node Comparison of the Split-Pipe and Discrete Problem

In this section we conduct two experiments. Namely, we compare

i) the split-pipe model (2) with the continuous relaxation of model (4) as two possible relaxations of the "original" discrete model (4),

ii) the split-pipe model (2) with the "original" discrete model (4).

We only processed the root node using the described test set to compare their dual bounds. To exploit the root node to a maximum extent, we aggressively apply separation in as many rounds as needed. We also aggressively apply OBBT, see [GBMW16], since tight variable bounds have an impact on the generation of tight cuts and thus on the dual bound. Furthermore, we disable all heuristics as well as strong branching, to avoid random noise.

For both experiments, we split the instances in two groups:

i) 25 out of 52 instances, where the discrete model could be solved to optimality within a timelimit of 5 hours. For these optimally solved instances, we compare the dual bound d of both relaxations after the root node with the optimal value p^* of the discrete model by means of $d/p^* \in [0, 1]$, denoted as "relative difference between dual bound in root node and optimal value" in the figures below. Note that all these 25 instances hold $p^* > 0$.

ii) 27 out of 52 instances, where the discrete model could not be solved to optimality within a timelimit of 5 hours.

Figure 9 shows that the dual bounds after solving the root node are better for the split-pipe model then for the continuous relaxation of the discrete model. A possible reason is that the continuous relaxation of the discrete model is weaker than the split-pipe model, because with the insights of section 3 and the computational results in table 5 of the appendix, we know that $X_{sp} \subsetneq X_{disc,rel}$.

Remember also that $X_{disc} \subseteq X_{sp}$ and thus the optimal value of the split-pipe model might be smaller than the optimal value of the discrete model. Hence the split-pipe model might not be able to close the gap of the discrete model in the root node.

However, the full discrete model yields better dual bounds in the root node compared to the split-pipe model as can be seen in figure 10, since the integer variables contain more information that can be exploited by for example presolving techniques, cutting planes or others.

5.4. Tree Experiment of the Split-Pipe and Discrete Problem

We conduct this experiment using the SCIP with default parameter settings. Again we split the instances in two groups:

i) 22 out of 52 instances that can be solved to optimality for both models (2) and (4),

ii) 30 out of 52 instances that are at the timelimit for at least one of both models.

Figure 11a reveals an important fact from the practical point of view. The optimal objective value of the split-pipe model is better than the one of the discrete model for all instances yielding pure cost savings when implementing the solution in practice. Remember that $X_{disc} \subseteq X_{sp}$ and thus the optimal value of the discrete model is always greater or equal than the one of the split-pipe model.

For example, the optimal solution of instance *belgium_240_1* is depicted in figure 13. It can be seen that partial loops may be optimal for the split-pipe model, while solutions of the discrete model only account for full loop lengths.

Figures 11b and 12 indicate that the runtime of the optimally solved instances as well as the remaining gap of the instances that are hit by the timelimit are better for the split-pipe model than for the discrete model. For the optimally solved instances (instances of type i), we use the shifted geometric mean as a performance measure. It is defined as $(\sqrt[n]{\prod(t_i + s)} - s)$ for values $t_1, ..., t_n$. We use a shift of $s = 10$ for the runtime and $s = 100$ for the number of branch and bound nodes in order to reduce the impact of

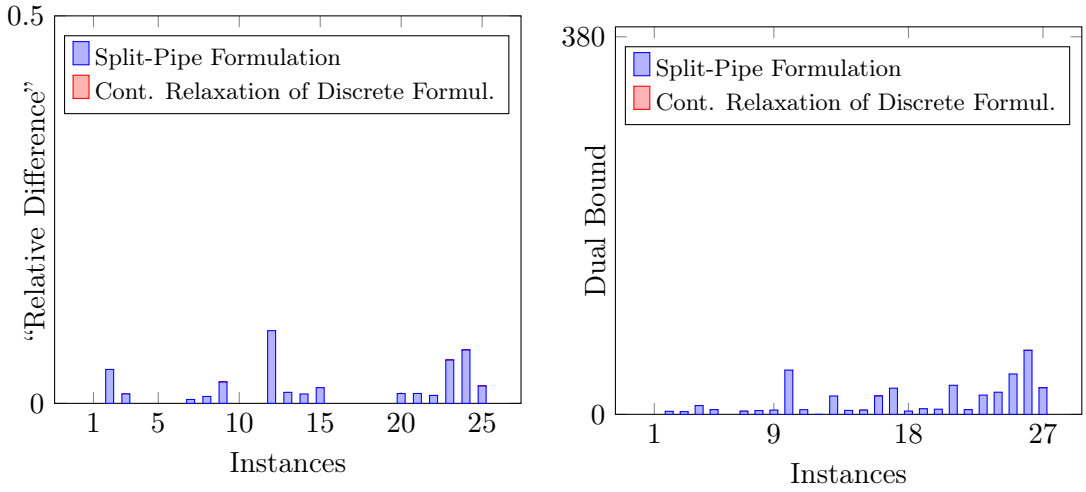

(a) "Relative difference" between dual bound in root node and optimal value for optimally solved instances.

(b) Dual bound in root node for not optimally solved instances

Figure 9: Root node experiment for split-pipe formulation versus continuous relaxation of discrete formulation.

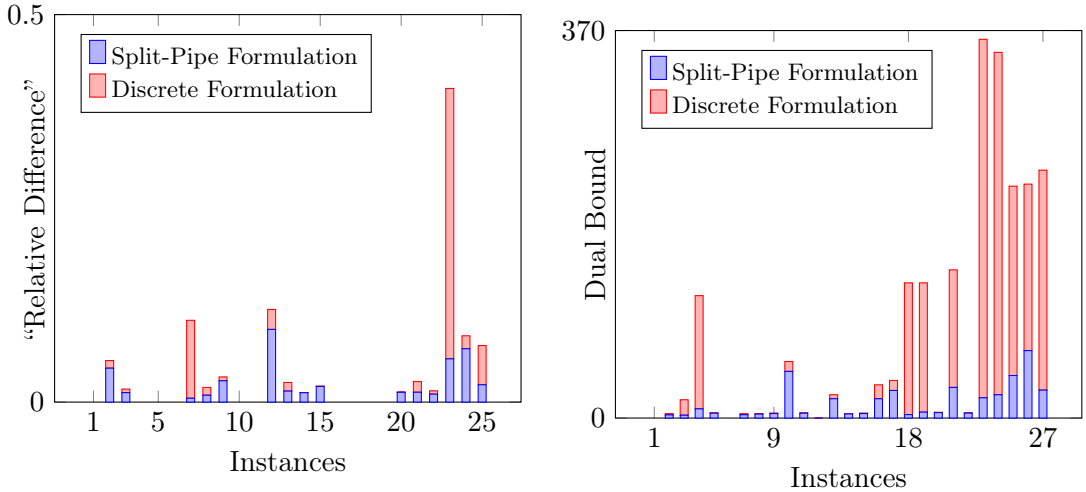

(a) "Relative difference" between dual bound in root node and optimal value for optimally solved instances.

(b) Dual bound in root node for not optimally solved instances.

Figure 10: Root node experiment for split-pipe formulation versus discrete formulation.

	Shifted Geometric Mean	
	Runtime in [sec]	Branch and Bound Nodes
Split-Pipe Problem	47.95	17145
Discrete Problem	372.91	83586

Table 1: Performance Values of optimally solved instances for the Split-Pipe and Discrete Problem.

very easy or hard instances in the mean values. Table 1 shows that the split-pipe problem outperforms the discrete problem with a factor of 7.78 concerning the runtime and with a factor of 4.88 with respect to the number of branch and bound nodes, which were needed to prove optimality.

This is due to several reasons, in particular, the relaxation of the discrete model is very weak as shown in the root node experiments. Take into account that the binary part comes along with big-M formulations and it is well known that their relaxations are weak. Besides, the LP-relaxation of the split-pipe model even finds solutions for these instances, which is very unlikely to happen in the discrete model.

The results in tables 3 and 4 show that no instance is infeasible for the discrete but feasible for the split-pipe model. Even though this observation suggests that each feasible solution of the split-pipe model might be transformable to a feasible solution of the discrete model we have seen in section 4.1 that this strongly depends on the given pressure bounds.

6. Summary

In the literature, different kind of network loop expansion approaches exist, in particular the discrete and the split-pipe problem. The question arises, whether there are significant differences between both problems, especially with respect to objective value and computation time.

To answer this question, we presented model formulations for the split-pipe and discrete loop expansion problems. We showed that the split-pipe model represents a relaxation of the discrete model and thus theoretically yields at least as good expansion solutions as the discrete model. But our computational study revealed that the split-pipe problem yields considerable better expansion costs than the discrete problem for instances that are solved to global optimality. This is of particular interest in practice, since implementing the split-pipe solutions yield pure cost savings over the discrete model.

On the other hand, it is worth mentioning that the optimal solution of the split-pipe problem can be retrieved by the discrete problem, because the split-pipe -argument says that an optimal solution contains at most two different equivalent diameters for a pipe. Thus splitting the pipe in two segments according to the optimal split-pipe solution yields

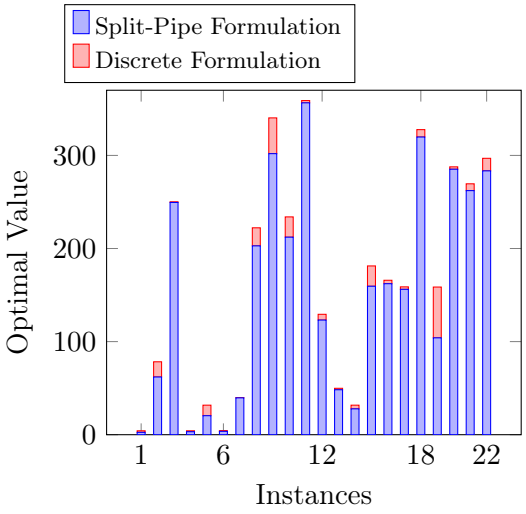

(a) Optimal value in [Mio €] of optimally solved instances for both models.

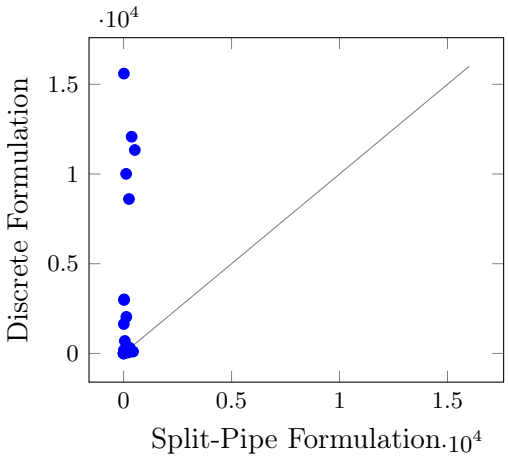

(b) Runtime in [sec] of optimally solved instances for both models.

Figure 11: Tree search experiment for split-pipe versus discrete formulation.

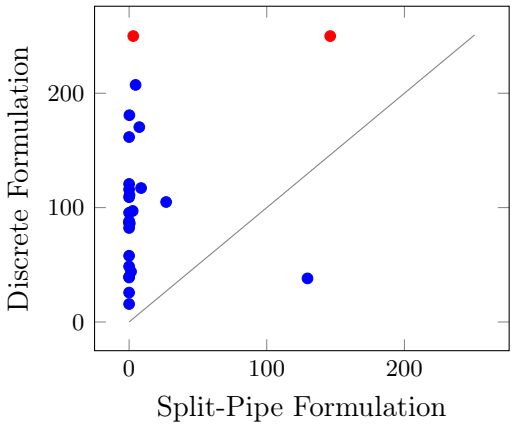

Figure 12: Gap in [%] of instances that are at the timelimit in the split-pipe and/or discrete formulation; red marked instances indicate that no primal bound has yet been found for the discrete formulation. For the best known upper and lower bounds U, L, the Gap $= (U - L)/L \cdot 100\%$.

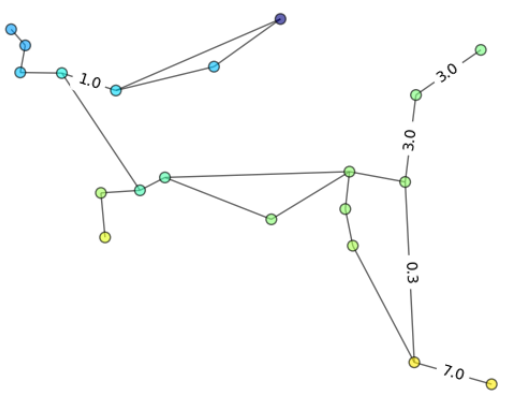

(a) Solution of split-pipe model.

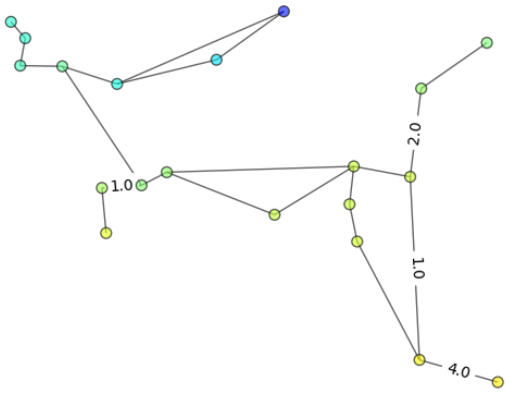

(b) Solution of discrete model.

Figure 13: Optimal solution of instance *belgium_240_1* for the split-pipe and discrete model in schematic view. The numbers i indicate the equivalent diameters $\hat{D}_{a,i}$ of the pipes, where pipes with diameter $\hat{D}_{a,0}$ are not displayed. Fractional values in the solution of the split-pipe model describe the proportion of the associated adjacent equivalent diameters, i.e. 0.3 means that 30% of that pipe corresponds to $\hat{D}_{a,1}$ and 70% to $\hat{D}_{a,0}$.

the same results for the discrete problem and requires only the addition of at most one inner node per pipe segment.

Acknowledgments

This work was supported by the *Research Campus Modal* funded by the German Federal Ministry of Education and Research (fund number 05M14ZAM).

A. Parallel Pipe Merge

When several pipes appear parallel to each other, every one is represented by a single Weymouth equation (1) in the model.

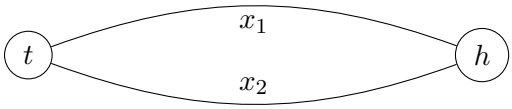

Figure 14: Parallel pipes.

For the two pipes in figure 14 we have the following system of equations:

$$p_t^2 - p_h^2 = \alpha x_1 |x_1| \tag{8}$$

$$p_t^2 - p_h^2 = \beta x_2 |x_2| \tag{9}$$

We transform this into an equivalent single equation for the summed (aggregated) flow $x = x_1 + x_2$. The new equation (10) is equivalent to (8), (9) in terms of the modeled gas physics, having a new weymouth constant, but the same pressure difference.

$$p_t^2 - p_h^2 = \gamma x |x| \tag{10}$$

Thus we have:

$$\alpha x_1 |x_1| = \beta x_2 |x_2| = p_t^2 - p_h^2 \stackrel{!}{=} \gamma x |x|$$

And we also know that $\text{sign}(x_1) = \text{sign}(x_2)$, since $\alpha, \beta > 0$.
Therefore,

$$\alpha x_1^2 = \beta x_2^2 \quad \Rightarrow \quad x_1 = \frac{\sqrt{\beta}}{\sqrt{\alpha}} x_2 \tag{11}$$

$$\stackrel{x = x_1 + x_2}{\Rightarrow} \quad x = (\frac{\sqrt{\beta}}{\sqrt{\alpha}} + 1) x_2 \tag{12}$$

$$\beta x_2^2 = \gamma x^2 \Rightarrow \quad \gamma = \frac{\beta x_2^2}{\left((\frac{\sqrt{\beta}}{\sqrt{\alpha}} + 1) x_2\right)^2} \tag{13}$$

$$\Rightarrow \quad \gamma = \frac{\beta}{\left(\frac{\sqrt{\beta} + \sqrt{\alpha}}{\sqrt{\alpha}}\right)^2} \tag{14}$$

$$\Rightarrow \quad \boxed{\gamma = \frac{\beta\alpha}{\left(\sqrt{\beta} + \sqrt{\alpha}\right)^2}} \tag{15}$$

B. Equivalent Diameters

For two parallel pipes (see figure 14) we can also compute an equivalent diameter value, using formula (11). Let

$$\alpha = \frac{KL}{D_1^5}, \qquad \beta = \frac{KL}{D_2^5}, \qquad \gamma = \frac{KL}{\hat{D}^5}$$

then

$$\gamma = \frac{\alpha\beta}{(\sqrt{\alpha} + \sqrt{\beta})^2}$$

$$\Leftrightarrow \quad \frac{KL}{\hat{D}^5} = \frac{\frac{KL}{D_1^5}\frac{KL}{D_2^5}}{\left(\sqrt{\frac{KL}{D_1^5}} + \sqrt{\frac{KL}{D_2^5}}\right)^2}$$

$$\Leftrightarrow \quad \frac{1}{\hat{D}^5} = \frac{\frac{1}{D_1^5 D_2^5}}{\left(\frac{1}{D_1^{5/2}} + \frac{1}{D_2^{5/2}}\right)^2}$$

$$\Leftrightarrow \quad (D_1^5 D_2^5)\left(\frac{1}{D_1^{5/2}} + \frac{1}{D_2^{5/2}}\right)^2 = \hat{D}^5$$
$$\Leftrightarrow \quad \boxed{\hat{D} = \left(D_1^{5/2} + D_2^{5/2}\right)^{2/5}}$$

C. Serial Merge

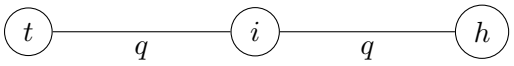

Figure 15: Serial pipes

In the situation of two pipes in serial, like in figure 15, we can also construct a single Weymouth equation equivalent to the original system. However, since the inner pressure variable p_i is eliminated, no bounds can be enforced now.

We start with:

$$p_t^2 - p_i^2 = \alpha q|q|$$
$$p_i^2 - p_h^2 = \beta q|q|$$

A simple linear combination already determines the coefficient:

$$p_t^2 - p_h^2 = (\alpha + \beta) q|q|$$
$$\Rightarrow \quad \boxed{\gamma = \alpha + \beta}$$

D. Computational Results

Instance	Dual Bound in [Mio €]		
	Discrete Model (4)	Continuous Relaxation of Discrete Model (4)	Split-Pipe Model (2)
belgium_100_1	0	0	0
belgium_100_2	4.2	0	3.43171814
belgium_110_1	4.2	5.09702375e-06	3.0598197
belgium_110_2	3.63797881e-14	0	0
belgium_120_1	0	0	0
belgium_120_2	0	0	0
belgium_130_1	4.2	0	0.199689463
belgium_130_2	4.2	0	1.98060027
belgium_140_1	0	0	0
belgium_140_2	4.2	0	3.01763531
belgium_150_1	4.2	8.33454766e-06	3.56329475
belgium_150_2	0	0	0
belgium_160_1	0	0	0
belgium_160_2	21.68	0	17.0026622
belgium_170_1	4.2	0	2.36123057
belgium_170_2	17.48	0	2.73106181
belgium_180_1	116.88	7.62076859e-05	8.81607249
belgium_180_2	4.2	0	4.13251234
belgium_190_1	4.8	0	4.73756269
belgium_190_2	0	0	0
belgium_200_1	4.8	3.91433035e-05	4.69945836
belgium_200_2	0	0	0
belgium_210_1	0	0	0
belgium_210_2	0	0	3.55271368e-15
belgium_220_1	4.20000001	5.62643699e-06	3.16825656
belgium_220_2	0	0	0
belgium_230_1	4.2	0	3.76671909
belgium_230_2	4.2	0	4.13025999
belgium_240_1	4.2	0	2.02227104
belgium_240_2	4.8	0	4.31106115
belgium_250_1	54	0	44.5426669
belgium_250_2	4.8	0	4.66326816
belgium_260_1	0	0	4.4408921e-15
belgium_260_2	22.28	0	18.4707778
belgium_270_1	4.2	0	2.95905216
belgium_270_2	4.2	0	3.93234996

continue next page

Instance	Dual Bound in [Mio €]		
	Discrete Model (4)	Continuous Relaxation of Discrete Model (4)	Split-Pipe Model (2)
belgium_280_1	4.8	2.18560156e-05	4.27848719
belgium_280_2	31.72	0.00273293657	18.4460988
belgium_290_1	109.08	0.000214055798	15.0590314
belgium_290_2	35.92	0	26.3421278
belgium_300_1	129.08	0	3.28565277
belgium_300_2	129.08	0	5.67457936
belgium_310_1	5.52	0	5.19578197
belgium_310_2	141.52	0	29.2440716
belgium_320_1	4.8	4.27249261e-05	4.7467948
belgium_320_2	22.28	0.000511436472	17.9327738
belgium_330_1	361.62121	0	19.3869623
belgium_330_2	21.68	7.4944901e-05	6.64494818
belgium_340_1	349.180328	0	22.2699238
belgium_340_2	221.4	0	40.6109587
belgium_350_1	223.35711	0.0103249313	64.3981751
belgium_350_2	236.661681	0.00117791695	26.7149075

Table 2: Root node experiment. Dual bound in root node of the discrete model and its two relaxations.

Instance	Dual Bound	Primal Bound	Gap%	Nodes	Time
belgium_100_1	4.2	4.2	0.0	11	0.5
belgium_100_2	78.32	78.32	0.0	15610	51.3
belgium_110_1	250.1	250.1	0.0	971432	1638.4
belgium_110_2	4.2	4.2	0.0	33	0.6
belgium_120_1	31.72	31.72	0.0	5562	21.9
belgium_120_2	4.2	4.2	0.0	10	0.5
belgium_130_1	39.8	39.8	0.0	18025	47.3
belgium_130_2	222.24	222.24	0.0	743915	2037.2
belgium_140_1	195.131067	308.14	57.9	>8827671	>18000.0
belgium_140_2	147.108893	276.7	88.1	>8608839	>18000.0
belgium_150_1	129.32	129.32	0.0	50784	104.7
belgium_150_2	49.84	49.84	0.0	61327	184.9
belgium_160_1	31.72	31.72	0.0	674	4.2
belgium_160_2	181.28	181.28	0.0	365326	694.9
belgium_170_1	165.88	165.88	0.0	1783993	2981.2
belgium_170_2	236.54743	326.68	38.1	>18079195	>18000.0
belgium_180_1	386.609255	447.4	15.7	>9332640	>18000.0
belgium_180_2	340.3	340.3	0.0	6306613	15597.3
belgium_190_1	233.96	233.96	0.0	27423	101.6
belgium_190_2	358.94	358.94	0.0	4202321	10008.4
belgium_200_1	335.732479	687.94	104.9	>7947916	>18000.0
belgium_200_2	280.92	280.92	0.0	2181875	5308.1
belgium_210_1	350.225023	773.1	120.7	>7787994	>18000.0
belgium_210_2	158.8	158.8	0.0	46259	102.0
belgium_220_1	258.927709	471.72	82.2	>9283627	>18000.0
belgium_220_2	327.7	327.7	0.0	5274875	11339.1
belgium_230_1	283.580154	528.32	86.3	>7624173	>18000.0
belgium_230_2	325.8	325.8	0.0	4028966	9548.7
belgium_240_1	158.6	158.6	0.0	1272525	3012.2
belgium_240_2	351.873667	920.82	161.7	>6298454	>18000.0
belgium_250_1	279.770489	589.91	110.9	>6195518	>18000.0
belgium_250_2	314.520029	438.88	39.5	>7552470	>18000.0
belgium_260_1	287.160951	623.52	117.1	>6429611	>18000.0
belgium_260_2	338.178808	1039.26	207.3	>5748824	>18000.0
belgium_270_1	287.72	287.72	0.0	5966250	12079.5
belgium_270_2	348.585474	438.1	25.7	>6807207	>18000.0
belgium_280_1	294.275986	437.26	48.6	>7106693	>18000.0
belgium_280_2	287.474906	399.18	38.9	>6651906	>18000.0

continue next page

Instance	Dual Bound	Primal Bound	Gap%	Nodes	Time
belgium_290_1	269.5	269.5	0.0	3540429	8606.5
belgium_290_2	304.525014	600.32	97.1	>9167402	>18000.0
belgium_300_1	356.847316	770.5	115.9	>6592294	>18000.0
belgium_300_2	324.950915	679.5	109.1	>7842075	>18000.0
belgium_310_1	439.676258	1189.04	170.4	>6101711	>18000.0
belgium_310_2	302.771894	436.1	44.0	>7166303	>18000.0
belgium_320_1	267.110222	522.08	95.5	>8937975	>18000.0
belgium_320_2	260.4	260.4	0.0	2068729	3634.7
belgium_330_1	509.353625	1430.5	180.8	>8804600	>18000.0
belgium_330_2	296.88	296.88	0.0	138776	315.9
belgium_340_1	615.722798	1e+20	–	>14588212	>18000.0
belgium_340_2	415.214085	1e+20	–	>10248912	>18000.0
belgium_350_1	388.794507	724.44	86.3	>8841363	>18000.0
belgium_350_2	428.808078	804.86	87.7	>6444757	>18000.0

Table 3: Tree experiment. Discrete model (4) using SCIP default parameter settings with a timelimit of 5 hours.

Instance	Dual Bound	Primal Bound	Gap%	Nodes	Time
belgium_100_1	2.52222139	2.52222139	0.0	11	1.5
belgium_100_2	61.9817718	61.9817718	0.0	139461	212.2
belgium_110_1	249.474608	249.474608	0.0	2961	9.4
belgium_110_2	3.18445469	3.18445469	0.0	35	2.3
belgium_120_1	20.4158615	20.4158615	0.0	53311	51.3
belgium_120_2	3.6289559	3.6289559	0.0	112	2.1
belgium_130_1	39.5729903	39.5729903	0.0	5962	11.0
belgium_130_2	202.835589	202.835589	0.0	53594	127.7
belgium_140_1	288.461258	288.461258	0.0	160577	283.4
belgium_140_2	263.563955	263.563955	0.0	1503402	1823.0
belgium_150_1	123.137348	123.137348	0.0	5699	16.5
belgium_150_2	48.290879	48.290879	0.0	6673	15.0
belgium_160_1	27.7657406	27.7657406	0.0	91	1.9
belgium_160_2	159.461633	159.461633	0.0	34238	57.4
belgium_170_1	162.200843	162.200843	0.0	9088	18.9
belgium_170_2	131.825355	302.6115	129.6	>3896341	>18000.0
belgium_180_1	444.155241	444.155241	0.0	4222483	6267.8
belgium_180_2	301.898355	301.898355	0.0	4465	14.9
belgium_190_1	212.171661	212.171661	0.0	3104491	4439.7
belgium_190_2	356.477864	356.477864	0.0	43261	117.5
belgium_200_1	505.683825	641.878072	26.9	>8024424	>18000.0
belgium_200_2	232.213875	271.101186	16.7	>8964972	>18000.0
belgium_210_1	691.634165	691.634165	0.0	728922	1270.4
belgium_210_2	156.151075	156.151075	0.0	20745	28.9
belgium_220_1	394.971073	394.971073	0.0	373035	652.3
belgium_220_2	319.753735	319.753735	0.0	2925988	5520.2
belgium_230_1	497.893409	497.893409	0.0	2087221	1069.9
belgium_230_2	216.21845	322.143883	49.0	>14442090	>18000.0
belgium_240_1	104.036519	104.036519	0.0	7205	25.8
belgium_240_2	726.221864	726.221864	0.0	150481	482.6
belgium_250_1	497.011878	498.61068	0.3	>10336785	>18000.0
belgium_250_2	420.681676	420.681676	0.0	125620	129.0
belgium_260_1	497.187518	540.375004	8.7	>4517080	>18000.0
belgium_260_2	729.190051	763.272131	4.7	>5545957	>18000.0
belgium_270_1	285.17026	285.17026	0.0	705740	1372.5
belgium_270_2	434.696853	434.696853	0.0	9141	22.4
belgium_280_1	395.568669	395.568669	0.0	1261661	1949.2
belgium_280_2	379.689853	379.689853	0.0	7159245	16248.7

continue next page

Instance	Dual Bound	Primal Bound	Gap%	Nodes	Time
belgium_290_1	262.191955	262.191955	0.0	188519	249.8
belgium_290_2	563.828834	578.324384	2.6	>7117122	>18000.0
belgium_300_1	718.665201	718.665201	0.0	1810824	6760.6
belgium_300_2	610.419044	610.419044	0.0	182039	414.9
belgium_310_1	915.860975	983.95377	7.4	>6274440	>18000.0
belgium_310_2	364.446337	369.605153	1.4	>11156408	>18000.0
belgium_320_1	505.169855	505.169855	0.0	219656	370.3
belgium_320_2	219.41697	251.257609	14.5	>6631372	>18000.0
belgium_330_1	1102.48954	1104.52468	0.2	>9223579	>18000.0
belgium_330_2	283.406916	283.406916	0.0	790395	1281.3
belgium_340_1	549.960326	1353.24302	146.1	>5597503	>18000.0
belgium_340_2	1054.21974	1085.77798	3.0	>4420102	>18000.0
belgium_350_1	684.491349	687.600538	0.5	>6264668	>18000.0
belgium_350_2	765.661839	765.661839	0.0	4999722	8862.4

Table 4: Tree experiment. Split-Pipe model (2) using SCIP default settings with a time-limit of 5 hours.

Instance	Objective value	
	Continuous Relaxation of Discrete Model	Split-Pipe Model
belgium_100_1	6.60586251e-05	2.52222139
belgium_100_2	6.22150924e-05	61.9817718
belgium_110_1	0.00190599563	249.474608
belgium_110_2	1.36978666e-05	3.18445469
belgium_120_1	0.000499125944	20.4158615
belgium_120_2	2.34692962e-05	3.6289559
belgium_130_1	0.000153166235	39.5729903
belgium_130_2	0.000321241063	202.835589
belgium_140_1	0.00176465756	288.461258
belgium_140_2	0.000825849983	263.563955
belgium_150_1	0.000275305383	123.137348
belgium_150_2	0.000363925487	48.290879
belgium_160_1	0.00288230767	27.7657406
belgium_160_2	0.000949544895	159.461633
belgium_170_1	0.000357317511	162.200843
belgium_180_1	0.0306389204	444.155241
belgium_180_2	0.0298727809	301.898355
belgium_190_1	0.0542993583	212.171661
belgium_190_2	0.0167594006	356.477864
belgium_210_1	0.0358858536	691.634165
belgium_210_2	0.00511362316	156.151075
belgium_220_1	0.0137327484	394.971073
belgium_220_2	0.0022300221	319.753735
belgium_230_1	0.116934571	497.893409
belgium_240_1	0.00247610046	104.036519
belgium_240_2	0.18070113	726.221864
belgium_250_2	0.0394282563	420.681676
belgium_270_1	0.00286603426	285.17026
belgium_270_2	0.101884114	434.696853
belgium_280_1	0.0434874474	395.568669
belgium_290_1	0.0140368277	262.191955
belgium_300_1	0.0239500904	718.665201
belgium_300_2	0.14461752	610.419044
belgium_320_1	0.064840339	505.169855
belgium_330_2	0.132093671	283.406916
belgium_350_2	0.350460766	765.661839

Table 5: Objective value of optimally solved instances for both the continuous relaxation of the discrete model and the split-pipe model.

References

[Ach09] Tobias Achterberg. SCIP: Solving constraint integer programs. *Mathematical Programming Computation*, 1(1):1–41, 2009.

[BBB+15] Conrado Borraz-Sánchez, Russell Bent, Scott Backhaus, Hassan L. Hijazi, and Pascal Van Hentenryck. Convex relaxations for gas expansion planning. *CoRR*, abs/1506.07214, 2015.

[BNV12] Frédéric Babonneau, Yurii Nesterov, and Jean-Philippe Vial. Design and operations of gas transmission networks. *Operations Research*, 60(1):34–47, 2012.

[Bra68] Dietrich Braess. Über ein Paradoxon aus der Verkehrsplanung. *Unternehmensforschung*, 12(1):258–268, 1968.

[DWS00] Daniel De Wolf and Yves Smeers. The gas transmission problem solved by an extension of the simplex algorithm. *Management Science*, 46(11):1454–1465, 2000.

[FD87] Okitsugu Fujiwara and Debashis Dey. Two adjacent pipe diameters at the optimal solution in the water distribution network models. *Water Resources Research*, 23(8):1457–1460, 1987.

[GBMW16] Ambros M. Gleixner, Timo Berthold, Benjamin Müller, and Stefan Weltge. Three enhancements for optimization-based bound tightening. *Journal of Global Optimization*, pages 1–27, 2016.

[HF15] Jesco Humpola and Armin Fügenschuh. Convex reformulations for solving a nonlinear network design problem. *Computational Optimization and Applications*, 62(3):717–759, 2015.

[HFK16] Jesco Humpola, Armin Fügenschuh, and Thorsten Koch. Valid inequalities for the topology optimization problem in gas network design. *OR Spectrum*, 38(3):597–631, 2016.

[Hum14] Jesco Humpola. *Gas network optimization by MINLP*. PhD thesis, Technische-Universität zu Berlin, 2014.

[KHPSe15] Thorsten Koch, Benjamin Hiller, Marc E. Pfetsch, and Lars Schewe (eds.). *Evaluating Gas Network Capacities*. MOS-SIAM Series on Optimization, 2015.

[Koc04] Thorsten Koch. *Rapid Mathematical Programming*. PhD thesis, Technische Universität Berlin, 2004. ZIB-Report 04-58.

[Lib] GAMS Model Library. General algebraic modeling system (GAMS) model library. `http://www.gams.com/modlib/modlib.htm`.

[Mau77] JJ Maugis. Etude de réseaux de transport et de distribution de fluide. *RAIRO - Operations Research - Recherche Opérationnelle*, 11(2):243–248, 1977.

[RMBS15] Roger Z Ríos-Mercado and Conrado Borraz-Sánchez. Optimization problems in natural gas transportation systems: A state-of-the-art review. *Applied Energy*, 147:536–555, 2015.

[Sza12] Jacint Szabó. The set of solutions to nomination validation in passive gas transportation networks with a generalized flow formula. Technical Report 11-44, Zuse Institute Berlin, 2012.

[Vig12] Stefan Vigerske. *Decomposition in Multistage Stochastic Programming and a Constraint Integer Programming Approach to Mixed-Integer Nonlinear Programming*. PhD thesis, Humboldt-Universität zu Berlin, 2012.

[Wey12] T. R. Weymouth. Problems in natural gas engineering. *Transactions of the American Society of Mechanical Engineers*, 34(1349):185–231, 1912.

[ZZ96] Jianzhong Zhang and Detong Zhu. A bilevel programming method for pipe network optimization. *SIAM Journal on Optimization*, 6(3):838–857, 1996.